This manuscript was accepted by Phys. Plasmas. Click here to see the version of record.

How Shear Increments Affect the Flow Production Branching Ratio in CSDX

J. C. Li[1] and P. H. Diamond[1]

[1]*CASS, University of California, San Diego, California 92093, USA*

Abstract

The coupling of turbulence-driven azimuthal and axial flows in a linear device absent magnetic shear (CSDX) is investigated. In particular, we examine the apportionment of Reynolds power between azimuthal and axial flows, and how the azimuthal flow shear affects axial flow generation and saturation by drift wave turbulence. We study the response of the energy branching ratio, i.e., ratio of axial and azimuthal Reynolds powers P_z^R/P_y^R, to incremental changes of azimuthal and axial flow shears. We show that increasing azimuthal flow shear decreases the energy branching ratio. When axial flow shear increases, this ratio first increases but then decreases to zero. The axial flow shear saturates below the threshold for parallel shear flow instability. The effects of azimuthal flow shear on the generation and saturation of intrinsic axial flows are analyzed. Azimuthal flow shear slows down the modulational growth of the seed axial flow shear, and thus reduces intrinsic axial flow production. Azimuthal flow shear reduces both the residual Reynolds stress (of axial flow, i.e., Π_{xz}^{Res}) and turbulent viscosity (χ_z^{DW}) by the same factor $|\langle v_y\rangle'|^{-2}\Delta_x^{-2}L_n^{-2}\rho_s^2c_s^2$, where Δ_x is the distance relative to the reference point where $\langle v_y\rangle = 0$ in the plasma frame. Therefore, the stationary state axial flow shear is not affected by azimuthal flow shear to leading order, since $\langle v_z\rangle' \sim \Pi_{xz}^{Res}/\chi_z^{DW}$.

This manuscript was accepted by Phys. Plasmas. Click here to see the version of record.

I. INTRODUCTION

Intrinsic flows of plasmas are beneficial to magnetic confinement and MHD control [1, 2]. Intrinsic flows occur both parallel to the magnetic field (e.g., toroidal rotations in tokamaks [3] and axial flows in linear devices [4]) and perpendicular to the magnetic field (e.g., zonal flows [5–7]). In particular, the combination of intrinsic parallel flow and weak magnetic shear is required for the formation of enhanced confinement states, such as states with de-stiffened heat flux profiles vs. ∇T [2]. Zonal flows are mesoscopic and can lead to the suppression of micro-turbulence [8]. Therefore, turbulence-driven flows at zero to weak magnetic shear are of interest. Controlled Shear Decorrelation Experiment (CSDX) is a linear device with comprehensive fluctuation and flow diagnostics and uniform axial magnetic fields, i.e., zero magnetic shear. In addition, the axial and azimuthal flows in CSDX are both driven by turbulence [4, 9, 10]. Thus, CSDX is an ideal venue to study the physics of turbulence-driven flows in uniform magnetic fields.

The generation of axial and zonal flows in CSDX can be viewed as a heat engine model [11], as illustrated by Fig. 1. Initially driven by profile gradients (e.g., ∇n_e in CSDX), the turbulence energy is coupled to both axial and zonal flows. Both flows are accelerated by Reynolds force, which is the gradient of Reynolds stress. The branching ratio of turbulent flow production is then the ratio of axial to azimuthal Reynolds powers. The Reynolds power is the product of Reynolds force and flow velocity, i.e., the axial Reynolds power is $P_z^R \equiv -\langle \tilde{v}_r \tilde{v}_z \rangle' \langle v_z \rangle$ and the azimuthal Reynolds power is $P_\theta^R \equiv -\langle \tilde{v}_r \tilde{v}_\theta \rangle' \langle v_\theta \rangle$. The branching ratio is then P_z^R / P_θ^R. In CSDX, the coupling of intrinsic axial and azimuthal (zonal) flows is weak, because $|k_z \langle v_z \rangle'| / k_\theta \langle v_\theta \rangle' \ll 1$ [4]. The turbulence energy is primarily coupled to zonal flows, i.e., $P_z^R / P_\theta^R \ll 1$. In return, zonal flows regulate drift wave turbulence through shearing. The axial flow is parasitic, riding on the drift wave–zonal flow system. Indeed, in the regime of intrinsic axial flows, the regulating effect of zonal flow is expected to be stronger than that of axial flow, due to weak axial flow shears, i.e., $|k_z \langle v_z \rangle'| / k_\theta \langle v_\theta \rangle' \ll 1$.

Intrinsic axial flows are driven by the axial Reynolds force, i.e., $-\langle \tilde{v}_r \tilde{v}_z \rangle'$. The axial Reynolds stress contains a diffusive component and a residual stress, i.e., $\langle \tilde{v}_r \tilde{v}_z \rangle = -\chi_z \langle v_z \rangle' + \Pi_{rz}^{Res}$. The residual stress does not depend on flow magnitude or shear, so the gradient of $-\partial_r \Pi_{rz}^{Res}$ accelerates the axial flow from rest. The residual stress requires spectral asymmetry in the k_θ–k_z space, because it is determined by the correlator $\langle k_\theta k_z \rangle \equiv \sum_k k_\theta k_z |\phi_k|^2$. In

FIG. 1: Schematic of turbulence-driven axial and azimuthal (zonal) flows in CSDX. P_z^R and P_θ^R are axial and azimuthal Reynolds powers, respectively.

CSDX, a seed axial flow shear breaks the spectral symmetry [12] without requiring the well-studied geometrical mechanisms [13, 14]. The residual stress then induces a negative viscosity increment, i.e., $\delta\Pi_{rz}^{Res} = -\chi_z^{Res}\delta\langle v_z\rangle'$, where $\chi_z^{Res} < 0$. When $|\chi_z^{Res}|$ exceeds the turbulent viscosity driven by drift waves—such that the total viscosity is negative—the seed flow shear is amplified by the modulational instability. The axial flow shear can saturate by two mechanisms. When the turbulent diffusion of axial momentum is equal to the residual stress in magnitude, the Reynolds stress and thus the axial Reynolds power are then zero, i.e., $\langle\tilde{v}_r\tilde{v}_z\rangle = 0$ and $P_z^R = 0$. As a result, the axial flow shear saturates. The saturated axial flow shear is determined by the balance between residual stress and the turbulent viscosity driven by drift waves, i.e., $\langle v_z\rangle' = \Pi_{rz}^{Res}/\chi_z^{DW}$. When the axial flow shear exceeds the linear threhold of parallel shear flow instability (PSFI) [15, 16], the strong, nonlinear turbulent viscosity induced by PSFI saturates the axial flow shear. The flow shear then saturates near and below the PSFI threshold [12], i.e., $|\langle v_z\rangle'| \lesssim |\langle v_z\rangle'|_{\rm crit}$.

Zonal flows are driven by vorticity flux. This is because the perpendicular Reynolds force is equivalent to vorticity flux, by the Taylor identity [17, 18], i.e., $-\langle\tilde{v}_r\tilde{v}_\theta\rangle' = -\langle\tilde{v}_r\tilde{\rho}\rangle$ where $\tilde{\rho} \equiv \nabla_\perp^2\tilde{\phi}$ is the vorticity. Consequently, the perpendicular Reynolds power is $P_\theta^R = -\langle\tilde{v}_r\tilde{\rho}\rangle\langle v_\theta\rangle$. Similar to the axial Reynolds stress, the vorticity flux contains a diffusive component and a residual flux, i.e., $\langle\tilde{v}_r\tilde{\rho}\rangle = -\chi_\theta\langle v_\theta\rangle'' + \Gamma_\rho^{Res}$ [7, 19]. While the generation of zonal flows is well-studied [5, 6], the question of what saturates the flow in the collisionless regime is seldom addressed. Recently, it has been shown that turbulent diffusion of vorticity saturates zonal flows, in absence of frictional drag [20, 21]. This new mechanism departs from the often-quoted saturation by tertiary instability of zonal flows [22]. The relevance of tertiary instability to zonal flow saturation in confinement devices is debatable.

The goal of this paper is to understand the evolution of fluctuation–flow ecology (including both $\langle v_\parallel\rangle$ and $\langle v_\theta\rangle$) [23, 24]. This has not been addressed by previous experiments or simulations. The question of what couples the parallel and perpendicular flows in absence of geometrical mechanisms is open. Magnetic shear allows perpendicular flow shears to break the symmetry of the $k_\parallel$ spectrum of turbulence, leading to the generation of intrinsic parallel flows [13]. However, this geometrical mechanism is not relevant for low or zero magnetic

shear, such as in the flat-q regime in tokamaks and linear devices with uniform magnetic fields, e.g., CSDX. The coupling of potential vorticity and parallel compression ($\nabla_\parallel \tilde{v}_\parallel$) can convert parallel flows into zonal flows [25]. But, this coupling is weak in the regime of intrinsic parallel flows, due to $k_\parallel L_n \ll 1$ in CSDX.

In this paper, we address the following questions:

(1) What is the branching ratio, i.e., the fraction of turbulence energy coupled to axial flows, relative to that coupled to zonal flows, in CSDX? In particular, we study how the increments of azimuthal and axial flow shears affect the branching ratio P_z^R/P_θ^R.

(2) How do zonal flow shears affect the generation and saturation of intrinsic axial flows, absent magnetic shear? In the context of CSDX, we study how the zonal flow shear affects the modulational instability of seed axial flow shear and the saturated axial flow shear.

We study the change of branching ratio in response to incremental changes of azimuthal and axial flow shears. We increase one of the azimuthal and axial flow shears, while fixing the other, and calculate the resulting branching ratio P_z^R/P_θ^R for each combination of axial and azimuthal flow shears. For each case, the flow profiles are fixed, i.e., we ignore the feedback of turbulence-generated flows on the flow profiles. By increasing the azimuthal flow shear, the change of P_z^R/P_θ^R reflects the competition between turbulence-driven axial and azimuthal flows. Increasing the axial flow shear allows us to explore the saturation of intrinsic axial flows. Particularly, we investigate whether the intrinsic axial flow shear saturates due to the turbulent viscosity driven by drift waves (χ_z^{DW}) or due to PSFI. This study addresses the regime where drift wave is the dominant instability population. Perpendicular Kelvin–Helmholtz (KH) instability driven by the azimuthal flow curvature is negligible [19], because KH drive is much weaker than the ∇n_0 drive, i.e., $|k_\theta \rho_s^2 \langle v_\theta \rangle''| \ll \omega_{*e}$. Here, $\omega_{*e} \equiv k_y \rho_s c_s / L_n$ is the electron drift frequency and $L_n \equiv n_0/|dn_0/dx|$ is the density gradient scale. As a result, we are interested in the regime where $|\langle v_\theta \rangle|/c_s \ll L_{V_\theta}^2/\rho_s L_n$, and L_{V_θ} is the scale length of azimuthal flow shear.

In addition, we study how azimuthal flow shears affect the generation and saturation of axial flows by turbulence. The axial residual stress is calculated including a strong azimuthal flow shear. We analyze the effect of azimuthal flow shears on the modulational instability of a seed axial flow shear. Moreover, study how the azimuthal flow shear affects the saturated

nal flow shear, which is calculated using $\langle v_z \rangle' = \Pi_{rz}^{Res}/\chi_z^{DW}$. Here, we consider the regime where PSFI is stable, i.e., $|\langle v_z \rangle'| \ll |\langle v_z \rangle'|_{\rm crit}$. Though the wave–flow resonance can be prominent in linear devices, here we consider the regime where the resonance is weak. In CSDX, where $|k_z|/k_\theta \ll 1$, the main resonance is between drift wave and azimuthal flow, i.e., $\omega_k - k_\theta \langle v_\theta \rangle - k_z \langle v_z \rangle \cong \omega_k - k_\theta \langle v_\theta \rangle \cong \omega_k - k_\theta \langle v_\theta \rangle' \Delta_x$. Δ_x is the distance relative to the reference position. The Doppler-shifted drift wave frequency is approximately $\omega_k \sim \omega_{*e}/(1 + k_\perp^2 \rho_s^2)$. Thus, when the value of $|k_\theta \langle v_\theta \rangle' \Delta_x|$ is close to ω_{*e}, the resonance is strong. In this work, we consider the regime where $|k_\theta \langle v_\theta \rangle' \Delta_x| \gg \omega_{*e}$, i.e., $|\langle v_\theta \rangle|/c_s \gg \rho_s L_{V_\theta}/\Delta_x L_n$. Hence, resonance is neglected. In addition, the KH drive is negligible compared to the drift wave drive, yielding $|\langle v_\theta \rangle|/c_s \ll L_{V_\theta}^2/\rho_s L_n$. Taken together, we focus on the regime where the azimuthal flow shear satisfies $\rho_s L_{V_\theta}/\Delta_x L_n \ll |\langle v_\theta \rangle|/c_s \ll L_{V_\theta}^2/\rho_s L_n$.

The rest of this paper is organized as follows: Section II presents how increments of azimuthal and axial flow shears affect the turbulence energy branching ratio. Section III studies the effects of azimuthal flow shear on the generation and saturation of intrinsic axial flows in CSDX. Section IV summarizes the main results. Section V discusses the results and future directions.

II. TURBULENCE ENERGY BRANCHING RATIO

We study the apportionment of turbulence energy between azimuthal and axial flows through a modulational study. We incrementally change the azimuthal or axial flow shear, while fixing the other, and study how the Reynolds work branching ratio P_z^R/P_θ^R changes respectively. Note in this study, we ignore the feedback of turbulence-driven flows on the flow profiles. Thus, the flow profiles are determined by external input, which is adjusted to match profiles from CSDX. In particular, we seek to answer the following questions:

(1) How do azimuthal flows compete for turbulence energy with axial flows?

(2) How do turbulence-driven axial flows saturate?

In the following, we present the results of this study.

We study the Hasegawa–Wakatani drift wave system coupled with parallel flow fluctuations in slab geometry in the presence of a mean perpendicular (azimuthal) flow $\langle v_y \rangle$ and a mean parallel (axial) flow $\langle v_z \rangle$, both of which vary in the $\hat{x}$ (radial) direction:

$$\frac{d}{dt}\tilde{n} + \tilde{v}_x \frac{\nabla n_0}{n_0} = D_\parallel \partial_z^2 (\tilde{n} - \tilde{\phi}) + D_c \nabla^2 \tilde{n}, \tag{1}$$

$$\frac{d}{dt}\tilde{\rho} + \tilde{v}_x \langle \rho \rangle' = D_\parallel \partial_z^2 (\tilde{n} - \tilde{\phi}) + \chi_c \nabla^2 \tilde{\rho}, \tag{2}$$

$$\frac{d}{dt}\tilde{v}_z + \tilde{v}_x \langle v_z \rangle' = -\partial_z \tilde{n}. \tag{3}$$

where we define $D_\parallel \equiv v_{The}^2/\nu_{ei}$ and $d/dt \equiv \partial_t + \langle v_y \rangle \partial_y + \langle v_z \rangle \partial_z$. ν_{ei} is electron–ion collision frequency and v_{The} is electron thermal speed. We have normalized electric potential fluctuation as $\tilde{\phi} \equiv e\delta\phi/T_e$ and density fluctuation as $\tilde{n} \equiv \delta n/n_0$, where n_0 is the equilibrium density. The magnetic field is uniform and lies in $\hat{z}$ direction. Both n_0 and $\langle v_y \rangle$ vary only in $\hat{x}$ direction. $\tilde{\rho} \equiv \rho_s^2 \nabla_\perp^2 \tilde{\phi}$ is the vorticity fluctuation, where ρ_s is the ion Larmor radius at electron temperature, $\langle \rho \rangle \equiv \langle v_y \rangle' \rho_s / c_s$ is the zonal vorticity where c_s is the ion sound speed. $\tilde{\mathbf{v}}_E \equiv c_s \hat{\mathbf{z}} \times \nabla \tilde{\phi}$ is the $E \times B$ velocity fluctuation. D_c and χ_c are the collisional particle diffusivity and vorticity diffusivity (i.e., viscosity).

Collisional drift waves are the dominant instability. The vorticity gradient may drive the perpendicular Kelvin–Helmholtz (KH) instability. But the vorticity gradient drive is quantitatively weaker than the ∇n_0 drive [19], i.e., $|k_y \rho_s^2 \langle v_y \rangle''|/\omega_{*e} \ll 1$ where $\omega_{*e} \equiv k_y \rho_s c_s / L_n$ is the electron drift frequency and $L_n \equiv n_0/|dn_0/dx|$ is the density gradient scale. Also, $|\langle v_z \rangle'|$ is well below the PSFI threshold, such that PSFI is strongly damped.

The azimuthal and axial flows are both externally imposed and fixed. We denote them as V_y and V_z to distinguish them from the intrinsic flows. As a result, the dispersion relation follows from the eigenmode equation for ϕ:

$$\rho_s^2 \frac{d^2\phi}{dx^2} = \left[k_y^2 \rho_s^2 - \frac{k_y \rho_s^2 V_y''}{\Omega_k} + \frac{i\alpha(\Omega_k - \omega_{*e})}{\Omega_k(\Omega_k + i\alpha)} + \frac{k_y k_z \rho_s c_s V_z'}{\Omega_k^2} - \frac{k_z^2 c_s^2 (\omega_{*e} + i\alpha)}{\Omega_k^2 (\Omega_k + i\alpha)} \right] \phi, \tag{4}$$

where $\alpha \equiv k_z^2 v_{The}^2/\nu_{ei}$ and $\Omega_k \equiv \omega_k - k_y V_y - k_z V_z + i\gamma_k$. We obtain the ϕ profile by using an eigenvalue solver. Here, we set the extent of the radial direction to be $0 \le x \le L_x$, where $L_x = 5\rho_s$. We set the parameters in the range relevant to CSDX, which are $\rho_s = 1$ cm, $L_n = 1.5$ cm, $k_y \rho_s = 0.7$, $L_z = 300$ cm, $k_z = -2\pi/L_z$. The adiabaticity parameter is $k_z^2 D_\parallel/\omega_{*e} = 3$. The flow profiles are: $V_y = V_{y,max} \sin[\pi(x/L_x - 0.5)]$ and $V_z = V_{z,max} \cos(\pi x/L_x)$. The boundary condition is $\phi(0) = \phi(L_x) = 0$. Then, we can obtain the drift wave frequency ω_k, growth rate γ_k, and ϕ profile.

This manuscript was accepted by Phys. Plasmas. Click here to see the version of record.

Using the ϕ profile, we determine the average Reynolds powers, which are: $P_y^R = -L_x^{-1}\int_0^{L_x} dx\partial_x\langle\tilde{v}_x\tilde{v}_y\rangle V_y$ and $P_z^R = -L_x^{-1}\int_0^{L_x} dx\langle\tilde{v}_x\tilde{v}_z\rangle' V_z$. By Taylor identity [17, 18], the azimuthal Reynolds force is identical to the vorticity flux, i.e., $-\partial_x\langle\tilde{v}_x\tilde{v}_y\rangle = -\langle\tilde{v}_x\tilde{\rho}\rangle$. Hence, the azimuthal Reynolds power becomes $P_y^R = -L_x^{-1}\int_0^{L_x} dx\langle\tilde{v}_x\tilde{\rho}\rangle V_y$. The vorticity flux contains a diffusive flux and a residual flux, i.e., $\langle\tilde{v}_x\tilde{\rho}\rangle = -\chi_y V_y'' + \Gamma_\rho^{Res}$. The azimuthal Reynolds power is then $P_y^R \sim L_x^{-1}\int_0^{L_x} dx\left[-\chi_y(V_y')^2 - \Gamma_\rho^{Res}V_y\right]$. Therefore, the turbulent diffusion of vorticity dissipates the azimuthal flow shear, because its contribution to P_y^R is negative definite. The residual vorticity flux can convert the turbulence energy to azimuthal flows, when $\Gamma_\rho^{Res}V_y < 0$. Similar to the vorticity flux, the axial Reynolds stress contains a diffusive momentum flux and a residual stress, i.e., $\langle\tilde{v}_x\tilde{v}_z\rangle = -\chi_z V_z' + \Pi_{xz}^{Res}$. Consequently, the axial Reynolds power is $P_z^R \sim L_x^{-1}\int_0^{L_x} dx\left[-\chi_z(V_z')^2 + \Pi_{xz}^{Res}V_z'\right]$. Thus, the residual stress can couple the turbulence energy to the axial flow, if $\Pi_{xz}^{Res}V_z' > 0$. The turbulent diffusion of axial momentum dissipates the axial flow.

The turbulent fluxes are calculated using the quasilinear theory. Here, we ignore the resonance between drift wave and the azimuthal and axial flows. Effects of resonance on regulating drift waves and zonal flow saturation are discussed in Ref. [20, 21]. As a result, the non-resonant turbulent diffusivity of vorticity is

$$\chi_y = \sum_{\omega_k \neq k_y V_y} \frac{|\gamma_k|}{|\Omega_k|^2} k_y^2\rho_s^2 c_s^2 |\phi_k|^2. \tag{5}$$

The residual vorticity flux is

$$\Gamma_\rho^{Res} = \sum_k k_y c_s^2 |\phi_k|^2 \left[\frac{|\gamma_k|\omega_{*e} + \alpha(\omega_{*e} - \Re\Omega_k)}{|\Omega_k + i\alpha|^2} - \frac{|\gamma_k|\omega_{*e}}{|\Omega_k|^2} + \Re\frac{i}{\Omega_k^2}k_z k_y \rho_s c_s V_z' - \Re\frac{ik_z^2 c_s^2(\omega_{*e} + i\alpha)}{\Omega_k^2(\Omega_k + i\alpha)}\right]. \tag{6}$$

The turbulent diffusivity of axial momentum is

$$\chi_z = \sum_k \frac{|\gamma_k|}{|\Omega_k|^2} k_y^2\rho_s^2 c_s^2 |\phi_k|^2. \tag{7}$$

The residual stress is

$$\Pi_{xz}^{Res} = \Re\sum_k \frac{ik_y k_z(\omega_{*e} + i\alpha)}{\Omega_k(\Omega_k + i\alpha)} \rho_s c_s^3 |\phi_k|^2. \tag{8}$$

FIG. 2: Change of branching ratio P_z^R/P_y^R in response to incremental changes of azimuthal flow shear. The axial flow profile is given by $V_z = V_{z,max}\cos(\pi x/L_x)$, where $V_{z,max} = 0.13c_s$. The azimuthal flow profile is given by $V_y = V_{y,max}\sin[\pi(x/L_x - 0.5)]$.

FIG. 3: Change of branching ratio P_z^R/P_y^R in response to incremental changes of axial flow shear. The axial flow profile is given by $V_z = V_{z,max}\cos(\pi x/L_x)$. The azimuthal flow profile is given by $V_y = V_{y,max}\sin[\pi(x/L_x - 0.5)]$, where $V_{y,max} = 0.13c_s$.

We study the changes of branching ratio of flow production by Reynolds work in response to incremental changes of azimuthal and axial flow shears. The branching ratio is the ratio of axial to azimuthal Reynolds powers P_z^R/P_y^R. It measures the turbulence energy apportionment between axial and azimuthal flows. Fig. 2 shows that azimuthal flow shear impedes the turbulent production of axial flow. When increasing the azimuthal flow shear, while fixing the axial flow, the ratio P_z^R/P_y^R decreases. This follows because the azimuthal flow shear reduces the magnitude of axial residual stress, i.e., $|\Pi_{xz}^{Res}|$ decreases. Because $P_z^R > 0$, the residual stress makes a positive contribution to P_z^R, i.e., $\Pi_{xz}^{Res}V_z' > 0$, in order to overcome the dissipation set by turbulent diffusion of axial momentum. Therefore, the axial Reynolds power decreases, as $|V_y'|_{max}$ increases.

Fig. 3 shows that the turbulent production of axial flow saturates below the PSFI threshold. We increase the axial flow magnitude $V_{z,max}$, with the azimuthal flow fixed. The ratio P_z^R/P_y^R first rises. For larger $V_{z,max}$, the ratio saturates and starts to decrease. Note that the saturation is *below* the PSFI threshold! Fig. 4 shows the drift wave growth rate vs. the axial flow shear. The onset of PSFI requires $|V_z'|_{max} > 2c_s/\rho_s$. The axial flow production saturates at $|V_z'|_{max} \cong 0.1c_s/\rho_s$, as given by Fig. 3, which is *far* below the PSFI threshold. This occurs because at $|V_z'|_{max} \cong 0.1c_s/\rho_s$, the turbulent diffusion of axial momentum is comparable to the residual stress in magnitude. This makes the axial Reynolds power close to zero, meaning that the net production of axial flows by turbulence approaches zero. As a result, the intrinsic axial flow shear saturates at $|V_z'|_{max} \cong 0.1c_s/\rho_s$, which is well below the PSFI threshold.

FIG. 4: Growth rate of drift wave instability for various axial flow shears. The axial flow profile is given by $V_z = V_{z,max}\cos(\pi x/L_x)$. The azimuthal flow profile is given by $V_y = V_{y,max}\sin[\pi(x/L_x - 0.5)]$, where $V_{y,max} = 0.13c_s$.

III. AZIMUTHAL FLOW EFFECTS ON INTRINSIC AXIAL FLOW

The intrinsic axial flow in CSDX is driven by drift wave turbulence, via a dynamical symmetry breaking mechanism [12]. In response to a seed axial flow shear, the residual Reynolds stress induces a negative viscosity increment. When this negative viscosity increment exceeds the turbulent viscosity driven by drift waves (i.e., such that the total viscosity is negative), the seed shear amplifies itself through a modulational instability.

When the axial flow shear steepens, a finite residual stress forms due to the spectral asymmetry of drift wave turbulence. The stationary profile of axial flow shear is then determined by the balance of residual stress with turbulent diffusion of axial momentum by drift waves, i.e. $\langle v_z\rangle' \sim \Pi_{xz}^{Res}/\chi_z^{DW}$.

In the rest of this section, we study the effects of azimuthal flow shear on the generation and saturation of axial flows. We first study how the azimuthal flow affects the stability of drift waves in CSDX. Then, we focus on how the azimuthal flow shear regulates the modulational instability of the seed axial flow shear. Also, we investigate how the azimuthal flow shear regulates the stationary axial flow shear profile determined by $\langle v_z\rangle' \sim \Pi_{xz}^{Res}/\chi_z^{DW}$.

A. Azimuthal flow effects on drift wave instability

We study the drift wave system described by Eqs. (1) to (3). Electrons are weakly adiabatic, i.e., $\tilde{n} = (1-i\delta)\tilde{\phi}$, where the non-adiabatic electron response $\delta < 1$. δ is determined by the frequency shift, i.e. $\delta = (\omega_{*e} - \omega_k - k_y\langle v_y\rangle - k_z\langle v_z\rangle)/k_z^2 D_\parallel$. The eigenmode equation is

$$\rho_s^2\frac{\partial^2\phi}{\partial x^2} = \left[\left(1+k_y^2\rho_s^2 - i\delta\right) - \frac{\omega_{*e}+k_y\rho_s^2\langle v_y\rangle''}{\Omega_k} + \frac{k_yk_z\rho_sc_s\langle v_z\rangle'}{\Omega_k^2} - (1-i\delta)\frac{k_z^2c_s^2}{\Omega_k^2}\right]\phi. \quad (9)$$

Multiplying both sides of Eq. (9) with ϕ^* and integrating over the radial direction, we obtain the linear dispersion relation, which is

$$\left(1+k_\perp^2\rho_s^2 - i\delta\right) - \frac{\omega_{*e}+k_y\rho_s^2\langle v_y\rangle''}{\Omega_k} + \frac{k_yk_z\rho_sc_s\langle v_z\rangle'}{\Omega_k^2} - (1-i\delta)\frac{k_z^2c_s^2}{\Omega_k^2} = 0. \quad (10)$$

Here, we define the effective radial wavenumber $k_x^2\rho_s^2 \equiv \rho_s^2\int_0^{L_x}dx|\partial_x\phi|^2/\int_0^{L_x}dx|\phi|^2$. Hence, the perpendicular wavenumber is $k_\perp^2\rho_s^2 \equiv k_x^2\rho_s^2 + k_y^2\rho_s^2$.

Azimuthal flows stabilize drift waves by reducing the effective electron drift frequency,

This manuscript was accepted by Phys. Plasmas. Click here to see the version of record.

which is $\overline{\omega_{*e}} \equiv \omega_{*e} + k_y\rho_s^2\langle v_y\rangle''$ in the presence of azimuthal flows. When the curvature of azimuthal flow satisfies $k_y\rho_s^2\langle v_y\rangle''/\omega_{*e} < 0$, the flow curvature weakens the effective electron drift frequency, and thus stabilizes. In CSDX, the condition $k_y\rho_s^2\langle v_y\rangle''/\omega_{*e} < 0$ holds true, and thus the azimuthal flow curvature stabilizes drift waves. In the following analysis, we consider the case where $k_y\rho_s^2\langle v_\theta\rangle''/\omega_{*e} < 0$. The Doppler-shifted frequency and linear growth rate of drift wave are calculated using the dispersion relation Eq. (10), which are

$$\omega_k \cong \frac{\overline{\omega_{*e}}}{1+k_\perp^2\rho_s^2} - \frac{k_y k_z \rho_s c_s \langle v_z\rangle'}{\overline{\omega_{*e}}}, \tag{11}$$

$$\gamma_k \cong \frac{1}{k_z^2 D_\parallel}\frac{\overline{\omega_{*e}}^2}{(1+k_\perp^2\rho_s^2)^2}\left(\frac{k_\perp^2\rho_s^2}{1+k_\perp^2\rho_s^2} - \frac{k_y\rho_s^2\langle v_y\rangle''}{\overline{\omega_{*e}}} + \frac{k_y k_z \rho_s c_s \langle v_z\rangle'}{\overline{\omega_{*e}}^2}\right). \tag{12}$$

The PSFI threshold for axial flow shear is:

$$|\langle v_z\rangle'|_{\rm crit} = \frac{1}{|k_y k_z \rho_s c_s|}\left[\frac{\overline{\omega_{*e}}^2(1+k_\perp^2\rho_s^2)}{4[(1+k_\perp^2\rho_s^2)^2+\delta^2]} + k_z^2 c_s^2\right]. \tag{13}$$

When exceeding the threshold given by Eq. (13), axial flow shear drives turbulence as a free energy source. Note that in the regime relevant to CSDX where $k_y\rho_s^2\langle v_y\rangle''/\omega_{*e} < 0$, the azimuthal flow lowers the PSFI threshold.

B. Azimuthal flow effects on axial residual stress

In this subsection, we show that azimuthal flow shear slows the modulational growth of the seed axial flow shear. Moreover, azimuthal flow shear reduces the magnitudes of both residual stress and turbulent viscosity. Consequently, the axial Reynolds power is reduced by azimuthal flow shear. Note this agrees with the trend shown in Fig. 2. However, azimuthal flow does not affect the stationary axial flow shear, to leading order. This follows because the axial flow is saturated by the turbulent viscosity. The effects of azimuthal flow shear cancels, to leading order, in determining the stationary axial flow shear, which is given by $\langle v_z\rangle' \sim \Pi_{xz}^{Res}/\chi_z^{DW}$.

First, we calculate the axial Reynolds stress with azimuthal flow effects included, following the same procedures presented in Ref. [12]. The axial Reynolds stress can be written as a

This manuscript was accepted by Phys. Plasmas. Click here to see the version of record.

diffusive momentum flux plus a residual stress, which is

$$\langle \tilde{v}_x \tilde{v}_z \rangle = -\chi_z \frac{\partial \langle v_z \rangle}{\partial x} + \Pi_{xz}^{Res}. \tag{14}$$

From Eq. (3), we obtain that

$$\tilde{v}_z \cong \frac{|\gamma_k|}{\left(\omega_k - k_y \langle v_y \rangle' \Delta_x\right)^2} k_z c_s^2 \tilde{\phi} \cong \frac{1}{(V'-1)^2} \frac{|\gamma_k|}{\omega_k^2} k_z c_s^2 \tilde{\phi}.$$

Here, $V' \equiv k_y \langle v_y \rangle' \Delta_x / \omega_k \sim \langle v_y \rangle \Delta_x L_n / c_s \rho_s L_{V_y}$. Thus, in the non-resonant regime (i.e., $|\langle v_y \rangle|/c_s \gg \Delta_x L_n / \rho_s L_{V_y}$, so $|V'| \gg 1$), we obtain that

$$\tilde{v}_z \sim \frac{1}{|V'|^2} \frac{|\gamma_k|}{\omega_k^2} k_z c_s^2 \tilde{\phi}. \tag{15}$$

As a result, the turbulent viscosity and residual stress are

$$\chi_z^{DW} \cong \sum_k \frac{1}{|V'|^2} \frac{1}{k_z^2 D_\parallel} \left[\frac{k_\perp^2 \rho_s^2}{1 + k_\perp^2 \rho_s^2} + \frac{|k_y \rho_s^2 \langle v_y \rangle''|}{\overline{\omega_{*e}}} \right] k_y^2 \rho_s^2 |\phi_k|^2, \tag{16}$$

$$\Pi_{xz}^{Res} \cong \sum_k \frac{1}{|V'|^2} \frac{1}{k_z^2 D_\parallel} (2 + k_\perp^2 \rho_s^2) \left[\frac{k_\perp^2 \rho_s^2}{1 + k_\perp^2 \rho_s^2} + \frac{|k_y \rho_s^2 \langle v_y \rangle''|}{\overline{\omega_{*e}}} + \frac{k_y k_z \rho_s c_s \langle v_z \rangle'}{\overline{\omega_{*e}}^2} \right] k_y k_z \rho_s c_s |\phi_k|^2. \tag{17}$$

The residual stress requires symmetry breaking in the k_y–k_z space. Note the 'negative viscosity piece in Eq. (17) (i.e., the third term in brackets, which is proportional to $k_y k_z \rho_s c_s \langle v_z \rangle'$) is negligible compared to the term proportional to $k_\perp^2 \rho_s^2/(1 + k_\perp^2 \rho_s^2)$ (i.e., the first term in brackets). Therefore, symmetry breaking in the k_y–k_z space is necessary for a nonzero Π_{xz}^{Res}. Absent magnetic shear, a seed axial flow shear breaks the symmetry and is self-amplified through a modulational instability. As a result, the broken symmetry in the k_y–k_z space emerges, along with a finite axial flow shear profile. Hence, with this spectral asymmetry, the residual stress, to leading order, is

$$\Pi_{xz}^{Res} \cong \sum_{k_y k_z \langle v_z \rangle' > 0} \frac{1}{|V'|^2} \frac{2 + k_\perp^2 \rho_s^2}{k_z^2 D_\parallel} \frac{k_\perp^2 \rho_s^2}{1 + k_\perp^2 \rho_s^2} k_y k_z \rho_s c_s I_k, \tag{18}$$

where $I_k = |\phi_k|^2 (k_y k_z \langle v_z \rangle' > 0) - |\phi_k|^2 (k_y k_z \langle v_z \rangle' < 0)$ accounts for the spectral imbalance. Therefore, both the residual stress and turbulent viscosity driven by drift waves are reduced

This manuscript was accepted by Phys. Plasmas. Click here to see the version of record.

by azimuthal flow shear. Consequently, the axial Reynolds power is reduced by azimuthal flow shear, yielding $P_z^R \sim |V'|^{-2}$. This agrees with the trend shown by Fig. 2.

Next, we show that the azimuthal flow shear also impedes the self-amplification of seed flow shear, i.e., azimuthal flow shear slows down the modulational growth of seed flow shear. In response to a seed axial flow shear $\delta\langle v_z\rangle'$, the residual stress induces a negative diffusion of momentum flux, i.e.,

$$\delta\Pi_{xz}^{Res} \cong |\chi_z^{Res}|\delta\langle v_z\rangle', \tag{19}$$

where the negative viscosity increment is

$$\chi_z^{Res} \cong -\frac{1}{|V'|^2}\frac{1}{D_\parallel}\frac{k_y^2\rho_s^2c_s^2}{\overline{\omega_{*e}}^2}\sum_k(1+k_\perp^2\rho_s^2)(4+k_\perp^2\rho_s^2)|\phi_k|^2. \tag{20}$$

The growth rate of the flow shear modulation is determined by the difference between $|\chi_z^{Res}|$ and χ_z, i.e.,

$$\begin{aligned}\gamma_q &= q_r^2(|\chi_z^{Res}| - \chi_z^{DW}) \\ &\cong q_r^2\sum_k \frac{|\phi_k|^2}{|V'|^2}\frac{k_y^2\rho_s^2c_s^2}{k_z^2D_\parallel}\left(K-\frac{k_\perp^2\rho_s^2}{1+k_\perp^2\rho_s^2}\right)\left(1+\beta\frac{|k_y\rho_s^2\langle v_y\rangle''|}{\omega_{*e}}\right),\end{aligned} \tag{21}$$

where q_r is the radial modenumber of the shear modulation, $K \equiv (1+k_\perp^2\rho_s^2)(4+k_\perp^2\rho_s^2)k_z^2c_s^2/\omega_{*e}^2$, and $\beta \equiv (2K-1)\Big/\left(K-\frac{k_\perp^2\rho_s^2}{1+k_\perp^2\rho_s^2}\right)$. When the negative viscosity induced by the residual stress exceeds the turbulent viscosity due to drift waves, the test flow shear is reinforced via modulational instability. This means $K > k_\perp^2\rho_s^2/(1+k_\perp^2\rho_s^2)$ is required for modulational growth (i.e., $\gamma_q > 0$) of the test shear. For drift waves, we obtain $k_y\rho_s \sim 1$, and thus $K \sim (2+k_x^2\rho_s^2)(5+k_x^2\rho_s^2) > 10k_z^2L_n^2$ and $0.5 < k_\perp^2\rho_s^2/(1+k_\perp^2\rho_s^2) < 1$. Modulational instability requires $K > k_\perp^2\rho_s^2/(1+k_\perp^2\rho_s^2) > 0.5$, which is possible for drift waves. As shown by Eq. (21), the modulational growth rate of the seed flow shear decreases when the azimuthal flow shear increases.

C. Azimuthal flow effects on stationary flow shear profile

The evolution of mean axial flow is described by

$$\frac{\partial\langle v_z\rangle}{\partial t}+\frac{\partial}{\partial x}\langle\tilde{v}_x\tilde{v}_z\rangle=-\frac{\partial P}{\partial z}-\nu_{ni}\left(\langle v_z\rangle-V_n\right). \tag{22}$$

The pressure drop in the axial direction is due to the heating on one end of the linear device. In CSDX, this pressure drop is weaker than the Reynolds force ($-\partial_x\langle\tilde{v}_x\tilde{v}_z\rangle$) by an order of magnitude [4]. Frictions between plasma and neutral flows damp the axial flow in the edge region, where neutral particles concentrate. Hence, neutral damping sets the boundary condition for the axial flow profile. Therefore, in the central region of CSDX, the axial flow is generated and saturated by the axial Reynolds stress. The stationary state flow is then determined by $\langle\tilde{v}_x\tilde{v}_z\rangle=0$. As a result, the stationary axial flow shear, to leading order, is

$$\langle v_z\rangle'=\frac{\Pi_{xz}^{Res}}{\chi_z^{DW}}\sim(2+k_\perp^2\rho_s^2)k_zc_s/k_y\rho_s. \tag{23}$$

The azimuthal flow shear reduces both Π_{xz}^{Res} and χ_z^{DW} by the same factor $|V'|^{-2}$. Hence, this reduction effect cancels out to leading order in the stationary axial flow shear, which is determined by the ratio $\Pi_{xz}^{Res}/\chi_z^{DW}$. Therefore, the azimuthal flow shear does not affect the saturated axial flow shear to leading order. Note the relation $\delta\Pi_{xz}^{Res}\propto\delta\langle v_z\rangle'$ is valid only for weak $\delta\langle v_z\rangle'$. As the axial flow shear grows larger, due to modulational instability, the residual stress is no longer linearly proportional to $\langle v_z\rangle'$. As shown by Fig. 3, when $\langle v_z\rangle'>0.05c_s/\rho_s$, the axial Reynolds power decreases with $\langle v_z\rangle'$, which means the residual stress is not linearly proportional to $\langle v_z\rangle'$. Therefore, $\langle v_z\rangle'=\Pi_{xz}^{Res}/\chi_z^{DW}$ can be used to calculate the saturated flow shear.

IV. SUMMARY OF MAIN RESULTS

In this work, we study the coupling of azimuthal and axial flows in CSDX, absent magnetic shear. We consider the regime of weak axial flow shear, such that V_z' is far below the PSFI threshold, i.e., $V_z'\ll|V_z'|_{\rm crit}$. In particular, we study how incremental changes of flow shears affect the production branching ratio P_z^R/P_y^R. Also, we investigate the effects of azimuthal flow shear on intrinsic axial flow generation and saturation, absent magnetic shear. The

main results are:

- Increasing azimuthal flow shear reduces the branching ratio, which is measured by the ratio of axial to azimuthal Reynolds powers, i.e., P_z^R/P_y^R.
- When axial flow shear increases, P_z^R/P_y^R first increases but then decreases to zero. P_z^R/P_y^R decreases because as axial flow shear increases, the turbulent diffusion of axial momentum approaches the axial residual stress in magnitude, such that the axial Reynolds stress decreases to zero. The intrinsic axial flow shear saturates at $|V_z'|_{max} \cong 0.1 c_s/\rho_s$, which is far below the PSFI threshold.
- When $k_y\rho_s^2\langle v_y\rangle''/\omega_{*e} < 0$, azimuthal flows stabilize drift waves by weakening the effective electron drift frequency $\overline{\omega_{*e}} \equiv \omega_{*e} + k_y\rho_s^2\langle v_y\rangle''$, so the drift wave growth rate is reduced by the azimuthal flow curvature.
- Azimuthal flow shear slows modulational growth of seed axial flow shear, and thus reduces the production of intrinsic axial flow, by shear suppression.
- Azimuthal flow shear reduces both axial residual stress (Π_{xz}^{Res}) and turbulent viscosity driven by drift waves (χ_z^{DW}) by the same factor, i.e., both Π_{xz}^{Res} and χ_z^{DW} scale with the azimuthal flow shear as $|V'|^{-2} \sim |\langle v_y\rangle'|^{-2}\Delta_x^{-2}L_n^{-2}\rho_s^2c_s^2$. So does the axial Reynolds power, i.e., $P_z^R \sim |V'|^{-2}$, which agrees with the trend that P_z^R/P_y^R decreases as azimuthal flow shear increases.
- Azimuthal flow shear does not affect the saturated axial flow shear to leading order, because $\langle v_z\rangle' = \Pi_{xz}^{Res}/\chi_z^{DW}$ and the reduction by $\langle v_y\rangle'$ cancels.

V. DISCUSSION

The results in this work can be used to develop testable predictions for simulation and experimental studies on interaction of parallel and perpendicular flows. This study is developed upon the regime with straight magnetic fields. This makes the results relevant to linear devices and flat-q regions in tokamaks. In tokamaks, the combination of weak magnetic shear (i.e., flat q profile) and strong toroidal rotation are required for the formation of enhanced confinement states [2], such as internal transport barriers. Thus, the turbulence

This manuscript was accepted by Phys. Plasmas. Click here to see the version of record.

energy apportionment between poloidal (i.e., zonal) and toroidal flows absent magnetic shear is of interest.

Further study on turbulence and flows in CSDX could include:

- Effects of extrinsic axial flows driven by axial momentum source on turbulence and intrinsic flows.
- Physics of transport barrier formation.

In the regime of intrinsic parallel flows, the feedback of axial flow shear on the turbulence–flow system is weaker than that of azimuthal flow shear in CSDX, because $|k_z V_z'/k_\theta V_\theta'| \ll 1$. As a result, *the turbulence is regulated primarily by V_θ', and axial flow is parasitic.* A non-parasitic axial flow regime is achievable with an external axial momentum source. Of course, when the enhanced axial flow shear exceeds the PSFI threshold, the resulting PSFI turbulence can drive zonal flow via strong acoustic coupling [25, 26]. Even below the PSFI threshold, externally driven axial flow shear can enhance the regulating effect of axial flow on turbulence. When $|k_z V_{z,tot}'|$ is comparable to $|k_\theta V_\theta'|$, the axial flow shear will have a strong effect on vorticity flux, mode structure, and fluctuation intensity. In both ways, the external axial momentum source can enhance the interaction of axial and azimuthal flows in CSDX. Moreover, the axial momentum source invokes the interaction of intrinsic and extrinsic axial flows, which is analogous to the 'cancellation' experiment [27]. This enables detailed studies on the modulational growth and saturation of seed axial flow shears in CSDX.

The external axial flow source allows us to explore the physics of transport barrier formation. Both strong toroidal rotation and weak magnetic shear are necessary for the formation of enhanced confinement states, e.g., states with internal transport barriers [2]. A linear device with zero magnetic shear and controlled axial flow shear–such as CSDX–is an ideal testbed to study the physics of such states. Increasing the axial flow shear can enhance zonal flow generation via the acoustic coupling [25, 26]. As a result, the enhanced zonal flow shear can lead to the formation of a transport barrier. In this way, we can study (1) what determines the axial flow shear threshold and (2) how the states of intrinsic axial flows evolve before and after the transition. These are important for understanding the dynamics of the flux-driven turbulence–zonal flow–axial flow ecology.

Acknowledgments

The authors are grateful to R. Hong and G. R. Tynan for inspiring and insightful discussions. We acknowledge useful and interesting discussions at the 9th Festival de Théorie in 2017. This work was supported by the U.S. Department of Energy, Office of Science, OFES, under Award Number DE-FG02-04ER54738.

---

[1] H. Reimerdes, T. C. Hender, S. A. Sabbagh, J. M. Bialek, M. S. Chu, A. M. Garofalo, M. P. Gryaznevich, D. F. Howell, G. L. Jackson, R. J. La Haye, et al., Physics of Plasmas **13**, 056107 (2006).

[2] P. Mantica, C. Angioni, C. Challis, G. Colyer, L. Frassinetti, N. Hawkes, T. Johnson, M. Tsalas, P. C. deVries, J. Weiland, et al., Phys. Rev. Lett. **107**, 135004 (2011).

[3] J. E. Rice, J. W. Hughes, P. H. Diamond, Y. Kosuga, Y. A. Podpaly, M. L. Reinke, M. J. Greenwald, O. D. Gürcan, T. S. Hahm, A. E. Hubbard, et al., Phys. Rev. Lett. **106**, 215001 (2011).

[4] R. Hong, J. C. Li, R. Hajjar, S. C. Thakur, P. H. Diamond, and G. R. Tynan, submitted to Physics of Plasmas (2018).

[5] P. H. Diamond, S. I. Itoh, K. Itoh, and T. S. Hahm, Plasma Physics and Controlled Fusion **47**, R35 (2005).

[6] Ö. D. Gürcan and P. H. Diamond, Journal of Physics A: Mathematical and Theoretical **48**, 293001 (2015).

[7] A. Ashourvan and P. H. Diamond, Phys. Rev. E **94**, 051202 (2016).

[8] H. Biglari, P. H. Diamond, and P. W. Terry, Physics of Fluids B: Plasma Physics **2**, 1 (1990).

[9] M. Xu, G. R. Tynan, P. H. Diamond, C. Holland, J. H. Yu, and Z. Yan, Phys. Rev. Lett. **107**, 055003 (2011).

[10] R. Hong, J. C. Li, S. C. Thakur, R. Hajjar, P. H. Diamond, and G. R. Tynan, submitted to Physical Review Letters (2018).

[11] Y. Kosuga, P. H. Diamond, and Ö. D. Gürcan, Physics of Plasmas **17**, 102313 (2010).

[12] J. C. Li, P. H. Diamond, X. Q. Xu, and G. R. Tynan, Physics of Plasmas **23**, 052311 (2016).

[13] Ö. D. Gürcan, P. H. Diamond, T. S. Hahm, and R. Singh, Physics of Plasmas (1994-present)

14, 042306 (2007).

[14] Ö. D. Gürcan, P. H. Diamond, P. Hennequin, C. J. McDevitt, X. Garbet, and C. Bourdelle, Physics of Plasmas **17**, 112309 (2010).

[15] N. Mattor and P. H. Diamond, Physics of Fluids **31**, 1180 (1988).

[16] J. C. Li and P. H. Diamond, Physics of Plasmas **24**, 032117 (2017).

[17] G. I. Taylor, Philosophical Transactions of the Royal Society of London. Series A, Containing Papers of a Mathematical or Physical Character **215**, 1 (1915).

[18] P. H. Diamond and Y. Kim, Physics of Fluids B: Plasma Physics **3**, 1626 (1991).

[19] A. Ashourvan, P. H. Diamond, and Ö. Gürcan, Physics of Plasmas **23**, 022309 (2016).

[20] J. C. Li and P. H. Diamond, submitted to Physical Review Letters (2018).

[21] J. C. Li and P. H. Diamond, submitted to Physics of Plasmas (2018).

[22] B. N. Rogers, W. Dorland, and M. Kotschenreuther, Phys. Rev. Lett. **85**, 5336 (2000).

[23] R. J. Hajjar, P. H. Diamond, A. Ashourvan, and G. R. Tynan, Physics of Plasmas **24**, 062106 (2017).

[24] R. J. Hajjar, P. H. Diamond, and G. R. Tynan, Physics of Plasmas **25**, 022301 (2018).

[25] L. Wang, P. H. Diamond, and T. S. Hahm, Plasma Physics and Controlled Fusion **54**, 095015 (2012).

[26] Y. Kosuga, S.-I. Itoh, and K. Itoh, Physics of Plasmas **24**, 032304 (2017).

[27] W. M. Solomon, K. H. Burrell, J. S. deGrassie, R. Budny, R. J. Groebner, J. E. Kinsey, G. J. Kramer, T. C. Luce, M. A. Makowski, D. Mikkelsen, et al., Plasma Physics and Controlled Fusion **49**, B313 (2007).

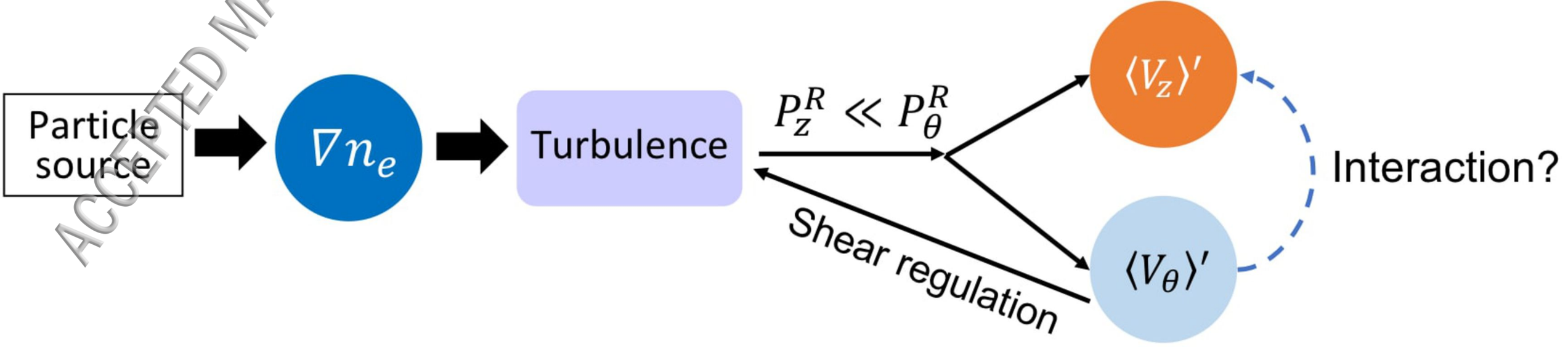
Particle source
∇n_e
Turbulence
$P_z^R \ll P_\theta^R$
$\langle V_z \rangle'$
$\langle V_\theta \rangle'$
Shear regulation
Interaction?